Talanta 113 (2013) 106–112

Contents lists available at SciVerse ScienceDirect

Talanta

journal homepage: www.elsevier.com/locate/talanta

Amplified cathodic electrochemiluminescence of luminol based on Pd and Pt nanoparticles and glucose oxidase decorated graphene as trace label for ultrasensitive detection of protein

Yaling Cao, Ruo Yuan *, Yaqin Chai *, Huijing Liu, Yuhong Liao, Ying Zhuo

Education Ministry Key Laboratory on Luminescence and Real-Time Analysis, College of Chemistry and Chemical Engineering, Chongqing 400715, People's Republic of China

ARTICLE INFO

Article history:
Received 12 December 2012
Received in revised form
6 March 2013
Accepted 7 March 2013
Available online 15 March 2013

Keywords:
Electrochemiluminescence
Luminol
Graphene
Glucose oxidase
Nanoparticles
Hydrogen peroxide

ABSTRACT

An ultrasensitive electrochemiluminescence (ECL) immunosensor was constructed for ultrasensitive detection of carcinoembryonic antigen (CEA) based on an amplified cathodic ECL of luminol at low potential. Firstly, Au nanoparticles (AuNPs) were electrodeposited onto single walled carbon nanotube–graphene composites (CNTs–Gra) coated glass carbon electrode (GCE) with enhanced surface area and good biocompatibility to capture primary antibody (Ab_1) and then bind the antigen analytes. Secondly, Pd and Pt nanoparticles (Pd&PtNPs) decorated reduced graphene oxide (Pd&PtNPs@rGO) and glucose oxidase (GOD) labeled secondary antibody (Pd&PtNPs@ rGO–GOD–Ab_2) could be captured onto the electrode surface by a sandwich immunoassay protocol to generate amplified cathodic ECL signals of luminol in the presence of glucose. The Pd&PtNPs@rGO composites and loaded GOD promoted luminol cathodic ECL response by efficiently catalyzing glucose to in-situ produce amount of hydrogen peroxide (H_2O_2) working as a coreactant of luminol. Then in turn Pd&PtNPs catalyzed H_2O_2 to generate various reactive oxygen species (ROSs), which accelerated the cathodic ECL reaction of luminol, enhanced the cathodic ECL intensity of luminol and improved the sensitivity of the immunosensor. The as-proposed ECL immunosensor exhibited sensitive response on the detection of CEA ranging from 0.0001 ng mL^{-1} to 160 ng mL^{-1} with a detection limit of 0.03 pg mL^{-1} (S/N=3). Moreover, the stability, specificity, lifetime and reproducibility tests demonstrated the feasibility of the developed immunoassay, which can be further extended to the detection of other disease biomarkers.

1. Introduction

Electrochemiluminescence or electrogenerated chemiluminescence (ECL) has become an attractive and powerful analytical technique in immunoassay [1,2], DNA analysis [3,4], environmental and food detection [5,6], and clinical and biomedical diagnostics [7,8]. Among them, ECL immunoassay has received considerable attention since it has the advantage of high sensitivity, wide dynamic concentration response range and good controllability [8,9]. Luminol or its derivatives, as one of the most commonly used ECL luminophores, were pointed out as efficient ECL systems as they could give out strong ECL emissions in the presence of reactive oxygen species (ROSs) [10]. Until now, most luminol-based sensors were studied based on luminol's anodic ECL and the peak potential position obtained at about 0.5 V (vs. Ag/AgCl) [11,12]. However, researchers concentrated little attention on the study of the cathodic ECL of luminol especially in the bioanalytical field. The main approach to trigger the cathodic ECL of luminol was hot electron induced ECL from thin oxide film-coated electrodes and semiconductor electrode [13]. A hot electron is an electron which is not in thermal equilibrium with the lattice; it occurs in the region of semiconductor device featuring high electric fields [14]. Nevertheless, hot electron-induced the cathodic ECL of luminol usually required not only high pulse voltage, but also some modification on the electrode interface [15]. It would be a challenging goal for us to obtain a sensitive and stable cathodic ECL signal of luminol and expand its application in the bioanalytical field by exploiting new materials and approaches.

Recently, nanostructure materials, not only as a good matrix for proteins but also as biological labels for immunoassay, have been developed rapidly to promote the progress of ECL biosensors due to their good biocompatibility, large surface area, excellent electrocatalytic activity, fascinating conductivity [4,16], and so on. For example, Guo et al. [4] constructed a strategy which integrated a DNA cycle device onto magnetic microbeads, amplifying the CdS NPs ECL signal with graphene oxide and achieving the sensitive detection for thrombin. Poly(diallyldimethylammonium chloride)-protected graphene–CdSe composites with high ECL intensity, good electronic conductivity, fast response, and satisfactory stability were prepared by Li et al. [16] for the sensitive detection of human IgG. Graphene, discovered by Novoselov in 2004 [17],

* Corresponding author. Tel.: +86 23 68252277; fax: +86 23 68253172.
E-mail addresses: yuanruo@swu.edu.cn (R. Yuan), yqchai@swu.edu.cn (Y. Chai).

0039-9140/$ - see front matter © 2013 Elsevier B.V. All rights reserved.
http://dx.doi.org/10.1016/j.talanta.2013.03.018

has become a rapidly rising star among carbon materials due to its excellent electronic transportation, large accessible surface area, and exceptional thermal conductivity and stability [18–20], driving the fascinating promise in the applications of catalytic supporting matrix for signal amplification of ECL biosensing [16,21]. Most importantly, a strong cathodic ECL emission of luminol was obtained at the graphene modified electrode due to the strong adsorption of dissolved oxygen by the graphene film [22]. However, compared with other nanomaterials, a key challenge is the prevention of aggregation of graphene in the practical application, which is of extraordinary importance for graphene because most of the unique properties are only associated with individual sheets [23]. To ameliorate this defect, a variety of functionalized graphenes have been formed by several techniques including the Scotch tape method, and non-covalent and covalent functionalization of reduced graphene oxide (rGO) [24–26]. Herein, introducing single walled carbon nanotubes (CNTs) into graphene as the electrode support matrix improved their electrochemical performances because tortuous and long CNTs could bridge the adjacent graphene sheet and inhibit the aggregation of graphene [27]. In addition, Pd and Pt nanoparticles (Pd&PtNPs) were modified on the surface of rGO to form Pd&PtNPs@rGO composites with satisfactory biocompatiblity, good conductivity and excellent electrocatalytic activity [28,29], which facilitate the immobilization of enzyme and secondary antibody with favorable catalysis activity and bioactivity.

In our study, we constructed an ultrasensitive sandwich-type immunosensor with CEA as the model analyte though amplifying the cathodic ECL of luminol. Concretely, AuNPs were electrodeposited on single walled carbon nanotube–graphene composites (CNTs–Gra) as sensor platform. On one hand, AuNPs and CNTs–Gra with fascinating conductivity and accelerating electronic transfer rate could motivate the cathodic ECL of luminol; on the other hand, AuNPs were a kind of excellent nanomaterial with favorable biocompatibility to immobilize primary antibody (Ab_1) and keep its bioactivity. Pd&PtNPs@rGO composites were used to load secondary antibody (Ab_2) and GOD. These composites and loaded GOD could improve the luminol cathodic ECL response by efficiently catalyzing glucose to in situ generate H_2O_2 as coreactant. Then in turn Pd&PtNPs catalyzed H_2O_2 to generate various ROSs, which accelerated the cathodic ECL reaction of luminol and then enhanced the luminol cathodic ECL intensity and improved the sensitivity of the immunosensor.

2. Experimental

2.1. Reagents and material

Graphene (Gra) and graphene oxide (GO) were obtained from Nanjing Xianfeng Nano Co. (Nanjing, China). Chitosan (Chi: MW ca. 1×10^6, >85% deacetylation), luminol (98%), glucose oxidase (GOD), and bovine serum albumin (BSA, 96%–99%) were bought from Sigma-Aldrich Co. (St. Louis, MO, USA). Chloroplatinic acid (H_2PtCl_6), potassium tetrachloropalladate (K_2PdCl_4), gold chloride tetrahydrate ($HAuCl_4\cdot4H_2O$) and sodium borohydride ($NaBH_4$) were purchased from Sinopharm Chemical Reagent Co. Ltd. (China). Carcinoembryonic antibody (Anti-CEA), carcinoembryonic antigen (CEA), fetoprotein antigen (AFP), and prostate specific antigen (PSA) standard solutions were obtained from Biocell (Zhengzhou, China). The serum samples were provided by Southwest Hospital (Chongqing, China). Poly(ethylenimine) (PEI, 50%) was received from Fluka (Switzerland). 1×10^{-2} M stock solution of luminol was prepared by dissolving luminol in 0.1 M NaOH solution and was kept at 4 °C when not in use. Phosphate buffer solutions (PBS) (pH 7.4) were prepared using 0.1 M Na_2HPO_4, 0.1 M KH_2PO_4 and 0.1 M KCl. Ferricyanide/ferrocyanide mixed solution ($Fe(CN)_6^{3-/4-}$, 5.0 mM, pH 7.4) was obtained by dissolving potassium ferricyanide and potassium ferrocyanide with PBS buffer (pH 7.4). All chemicals and solvents used were of analytical grade and were used as received without further purification. Double-distilled water was used throughout this study.

2.2. Apparatus

The ECL measurements were monitored with a model MPI-A electrochemiluminescence analyzer (Xi'An Remax Electronic Science & Technology Co. Ltd., Xi'An, China) with the voltage of the photomultiplier tube (PMT) set at 800 V and the applied potential 0–0.4 V (vs. Ag/AgCl) during detection. Cyclic voltammetric (CV) measurements were carried out on a CHI 610A electrochemistry workstation (Shanghai CH Instruments, China). All experiments were performed with a conventional three-electrode system. Platinum wire, saturated Ag/AgCl electrode and modified glassy carbon electrode (GCE $\Phi=4$ mm) were used as the auxiliary electrode, reference electrode and working electrode, respectively. X-ray photoelectron spectroscopy (XPS) measurement was operated on a VG Scientific ESCALAB 250 spectrometer (Thermoelectricity Instruments, USA) using Al Kα X-ray (1486.6 eV) as the light source. Scanning electron micrographs were taken with a scanning electron microscope (SEM, S-4800, Hitachi). Transmission electron microscopy (TEM) images were acquired by a transmission electron microscope (TEM, TECNAI 10, Philips Fei Co., Hillsboro, OR). pH measurements were made with a pH meter (MP 230, Mettler-Toledo, Switzerland) and a digital ion analyzer (Model PHS-3C, Dazhong Instruments, Shanghai, China).

2.3. Preparation of Pd and Pt nanoparticles decorated rGO nanocomposites (Pd & PtNPs@rGO)

The rGO was prepared according to Reference [30] with a minor modification in supplementary material. The resulting rGO, with abundant amino on its surface due to the presence of PEI, was then surface-chemically modified by metal nanoparticles. Pd&PtNPs decorated rGO (Pd & PtNPs@rGO) composites were obtained using $NaBH_4$ as a reducing agent. Briefly, a mixed aqueous solution contained 1 mL H_2PtCl_6 (0.5%) and 1 mL K_2PdCl_4 (0.5%) was added dropwise into 2 mL as-synthesized rGO with the aid of ultrasonic agitation for several minutes, which made the negatively charged $PdCl_4^{2-}$ and $PtCl_6^{2-}$ ions adsorb onto the rGO surface. Subsequently, 1 mL $NaBH_4$ (0.1 M) solution was added into the mixture drop by drop with ultrasonic agitation for 20 min. The product was collected by centrifugation and washed several times with double distilled water. It was stored in the refrigerator at 4 °C when not in use.

2.4. Preparation of Ab_2 and GOD-labeled Pd & PtNPs@rGO (Pd & PtNPs@rGO–GOD–Ab_2 bioconjugates)

The Pd&PtNPs@rGO–GOD–Ab_2 bioconjugates were synthesized according to the following steps. Anti-CEA solution with 0.2 mL was added slowly to 2 mL of the as-prepared Pd&PtNPs@rGO suspension under soft stirring at 4 °C for 4 h. Subsequently 1 mL of GOD (1 mg mL^{-1}) was added into Pd&PtNPs@rGO labeled Ab_2 suspension and incubated at 4 °C for 4 h to block the unspecified binding sites and prevent non-specific adsorption. Then, free antibodies and GOD were removed by centrifugation and the resulting precipitates were washed with PBS several times to obtain Pd&PtNPs@rGO–GOD–Ab_2 bioconjugates. Finally, the resultant bioconjugates were redispersed in PBS (pH 7.4) and stored at 4 °C for further use. The entire process for construction of the Pd&PtNPs@rGO–GOD–Ab_2 bioconjugates is illustrated in Fig. 1B.

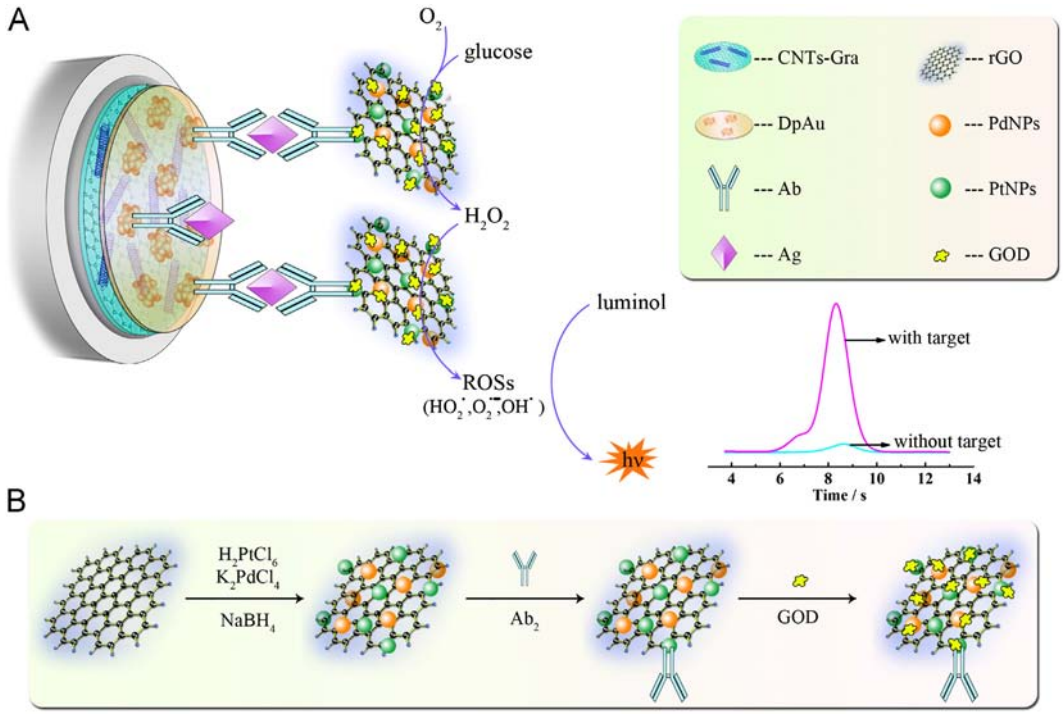

Fig. 1. (A) The fabrication process of the proposed immunosensor and the mechanism of detection for CEA; (B) the preparation procedure of Ab_2 and GOD labeled Pd & PtNPs@rGO.

2.5. Fabrication of the ECL immunosensor

Prior to modification, the GCE (Φ=4 mm) was polished with 0.3 μm and 0.05 μm alumina slurry to obtain a mirror-like surface, and then ultrasonically cleaned with ethanol and water. 1 mg graphene and 1 mg CNTs were dispersed in 2 mL of 0.5% chitosan solution to obtain CNTs–Gra homogeneous suspension by sonication. The pretreated GCE was firstly coated with 6 μL CNTs–Gra composites (abbreviated as CNTs–Gra/GCE) and allowed to dry in air. Then the electrode was immersed into 1% $HAuCl_4$ solution to form nano-Au layer (abbreviated as DpAu/CNTs–Gra/GCE) via potentiostatic electrodeposition for 30 s at −0.2 V. Next, the obtained electrode was submerged into Ab_1 (anti-CEA) solution at 4 °C for 4 h (abbreviated as Ab_1/DpAu/CNTs–Gra/GCE) to immobilize Ab_1 via the tight chemical function, originating from the binding of thiol groups and amino groups from cysteine residues that exist in the proteins to the Au surface. Following that, 20 μL of 1% BSA solution was placed onto the electrode for 30 min at room temperature to eliminate non-specific binding effects and block the remaining active sites (abbreviated as BSA/Ab_1/DpAu/CNTs–Gra/GCE). The modified electrode was thoroughly cleaned with PBS (pH 7.4) to remove the non-chemisorbed species after every modificatory step. Thus the proposed immunosensor was constructed successfully and stored at 4 °C for CEA detection. Fig. 1A shows the schematic illustration of the immunosensor fabrication process.

2.6. Measurement procedure of CEA

Based on the typical process of sandwich immunoassay, the obtained immunosensors were incubated with different concentrations of CEA standard antigen (Ag) solution for 20 min at room temperature followed by washing thoroughly with PBS (pH 7.4). Whereafter, Ag/BSA/Ab_1/DpAu/CNTs–Gra modified GCE was further incubated with Pd&PtNPs@rGO–GOD–Ab_2 bioconjugates for sandwich immune reaction. After rinsing thoroughly with PBS to remove the unbound secondary antibody, the immunosensors with different concentrations of CEA were placed into an ECL detector cell containing 3 mL PBS with 1×10^{-4} M luminol and an appropriate concentration of glucose to record ECL signals at room temperature. The measurements of clinical serum samples were performed with the same procedures mentioned above without any other treatments.

3. Results and discussion

3.1. Characteristics of the different nanomaterials

The surface images of the CNTs–Gra and DpAu/CNTs–Gra composite membranes were investigated by using SEM. As shown in Fig. 2A, the CNTs and graphene dispersed by chitosan showed that the CNTs were successfully introduced into graphene and displayed a homogeneous configuration and good dispersion. After AuNPs were electrodeposited onto the CNTs–Gra film, we could see that the size of AuNPs was ranging from 100 nm to 400 nm (Fig. 2B). This 3-D structure made the composite film become more porous rougher. Such a layer presented a large specific surface area and good biocompatibility for further immobilization of antibody.

To verify the successful synthesis of rGO and Pd&PtNPs@rGO, TEM measurement was employed to gain the morphology of the as synthesized composites. Fig. 2C and D displays the TEM images before and after the rGO was modified with Pd&PtNPs. The lamellate mono-layer sheets could be observed clearly in Fig. 2C, suggesting the successful preparation of rGO for further functionalization. Compared with the rGO, the homogeneous coverage of Pd&PtNPs on the graphene surface with a size of about 30 nm could be found in Fig. 2D.

To further analyze the chemical composition of the Pd&PtNPs@rGO nanocomposites, XPS characterization was employed. As expected, the XPS characteristic peaks for Pt4f, Pd3d, C1s, N1s and O1s core level regions could be obviously observed at the Pd&PtNPs@rGO composites in Fig. 2E. The peak at 284.6 eV (Fig. S1A) could be assigned to C1s XPS

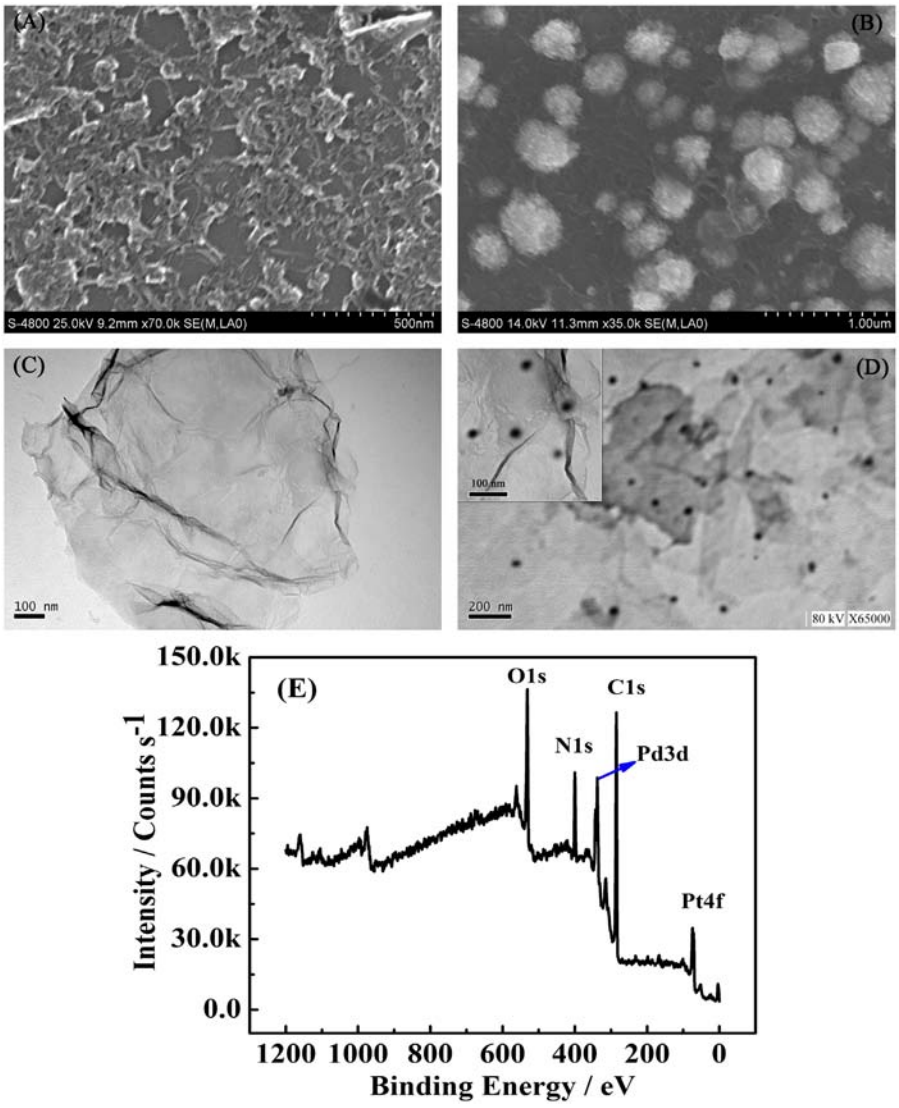

Fig. 2. SEM images of (A) CNTs–Gra nanocomposites and (B) DpAu/CNTs–Gra; TEM images of (C) rGO and (D) Pd&PtNPs@rGO; and (E) XPS of Pd&PtNPs@rGO nanocomposites.

spectra, which testified to the presence of rGO together with O1s at 531.4 eV. The peak of N1s at 400.0 eV (Fig. S1B) clearly demonstrated the existence of N element in the composites. The presence of N1s spectra originated from PEI, which was beneficial to further modification with metal nanoparticles. The Pd3d doublet features with binding energies of 343.2 eV and 338.2 eV are presented in Fig. S1C, suggesting the presence of the PdNPs. Fig. S1D represents the core level spectrum of the Pt4f doublet with binding energies of 71.4 eV and 74.5 eV which confirmed the formation of metallic Pt. These results indicated that the Pd&PtNPs@rGO composites have been successfully prepared.

3.2. CV characterization of the ECL immunosensor

CV is a useful technology to probe the process of electrode modification. Fig. 3A depicts the CVs of different modified electrodes in 5 mM $Fe(CN)_6^{4-/3-}$ solution in PBS of pH 7.4 containing 0.1 M KCl from −0.2 V to 0.6 V (vs. SCE) at a scan rate of 100 mV s^{-1}. From the image, we can see that the current of CNTs–Gra (curve b) and DpAu/CNTs–Gra (curve c) modified electrode increased step by step compared with bare GCE (curve a), which is attributed to the excellent conductivity of CNTs–Gra nanocomposites and AuNPs. When the antibody was immobilized on DpAu/CNTs–Gra/GCE, the response current decreased (curve d) because the antibody biomacromolecules acting as a nonconductor could obstruct the electron transfer toward the electrode surface. Subsequently, the resulting electrode was blocked with 1% BSA (curve e) and then incubated with CEA antigen (curve f), and the stepwise decrease of CV responses was observed. The reason for this was that the insulating BSA and CEA protein layers on the electrode retard the interfacial electron transfer.

3.3. ECL characterization of modified electrodes

The ECL performances of the immunosensor were characterized step by step and the corresponding ECL intensity–time curves of the modified electrode are shown in Fig. 3B, executed in 0.1 M PBS (pH 7.4) containing 1×10^{-4} M luminol and appropriate glucose. And all these results were recorded until the electrode had reached a steady-state response. As shown in this figure, no detectable ECL signals could be found for the bare GCE (curve a) at a scanning potential from 0.0 V to 0.4 V. When the bare GCE was modified with CNTs–Gra composites, a distinguished and stable cathodic ECL peak appeared at about 0.05 V (curve b), ascribed to the strong adsorption of dissolved trace O_2 and the excellent electrocatalytic properties of graphene that facilitated the reduction of dissolved trace O_2 to form ROSs such as $HO_2\bullet$, $O_2\bullet^-$ and OH•, which motivated the

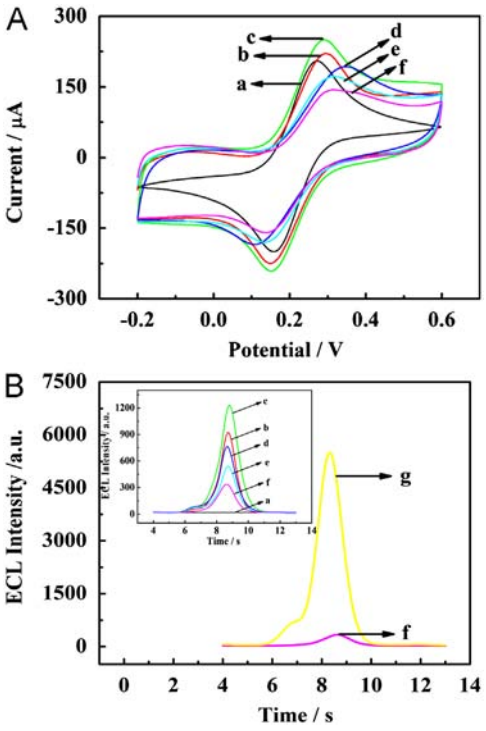

Fig. 3. (A) CVs for bare GCE (a), CNTs–Gra (b), DpAu/CNTs–Gra (c), Ab_1/DpAu/CNTs–Gra (d), BSA/Ab_1/DpAu/CNTs–Gra (e), and Ag/BSA/Ab_1/DpAu/CNTs–Gra (f) modified GCE in 5 mM $K_3[Fe(CN)_6]/K_4[Fe(CN)_6]$ (1:1) solution (pH 7.4) containing 0.1 M KCl at 100 mV s^{-1}. (B) Inset: the ECL responses of bare (a), CNTs–Gra (b), DpAu/CNTs–Gra (c), Ab_1/DpAu/CNTs–Gra (d), BSA/Ab_1/DpAu/CNTs–Gra (e), and Ag/BSA/Ab_1/DpAu/CNTs–Gra (f) modified GCE. The ECL responses of Ag/BSA/Ab_1/DpAu/CNTs–Gra modified GCE before (f) and after (g) incubating with Pd&PtNPs@rGO–GOD–Ab_2. All working buffers were 0.1 M PBS (pH 7.4) containing 1×10^{-4} M luminol and 0.01 M glucose.

cathodic ECL reaction of luminol [27,28,31]. Subsequently, a further increase of ECL intensity was observed after AuNPs were assembled to CNTs–Gra/GCE (curve c). The reason may be that the AuNPs played an important role similar to a conducting wire, which made the electron transfer easier in a luminol-based cathodic ECL reaction. Then the ECL intensity dropped with the immobilization of Ab_1 (curve d), blocking with BSA (curve e) and incubation with CEA antigen (curve f) because of the formation of less conductive layers, which slowed down the electron transfer speed in luminol ECL reactions significantly and led to the decrease of ECL signal. After the Ag/BSA/Ab_1/DpAu/CNTs–Gra modified electrode was incubated with Pd&PtNPs@rGO–GOD–Ab_2 bioconjugates solution for immune reaction to obtain the proposed immunosensor, the ECL signal was improved considerably (curve g), and the possible mechanism is shown in Fig. 1.

3.4. Optimization of analytical conditions

The concentration of glucose in the detection buffer had an important influence on the analytical performance of the proposed ECL immunosensor. As seen in the ECL response of the proposed immunosensor shown in Fig. S2, the ECL intensity increased sharply with the increasing concentration of glucose up to 0.01 M and then tended to level off. Thus, the optimum concentration of glucose employed was 0.01 M for the determination of CEA.

3.5. Comparison of the immunosensors using different labeled probes

Fig. 4 showed the ECL–time curves of different labeled probes, which were used for the detection of the same concentration analyte by the same assay protocol, including Pd&PtNPs@rGO–GOD–Ab_2 bioconjugates (curve a), PdNPs@rGO–GOD–Ab_2 bioconjugates (curve b), PtNPs@rGO–GOD–Ab_2 bioconjugates (curve c) and rGO–GOD–Ab_2 bioconjugates (curve d). It should be noticed that the ECL signal from Pd&PtNPs@rGO–GOD–Ab_2 bioconjugates exhibited much higher ECL response than those obtained from three other labeled probes, indicating that the Pd&PtNPs@rGO–GOD–Ab_2 probe could greatly amplify the ECL signal. The reasons may be that on the one hand, the large numbers of Pd&PtNPs coated on the rGO could greatly improve the loading amount of GOD and Ab_2 molecules, which could result in a higher catalytic efficiency for glucose to in situ produce H_2O_2; on the other hand, Pd&PtNPs displayed a greater catalytic efficiency than PdNPs and PtNPs only for H_2O_2 to generate various ROSs, which could accelerate the reaction of luminol to form 3-aminophthalate anions at the excited state and then enhance the luminol ECL intensity. Therefore, Pd&PtNPs@rGO–GOD–Ab_2 bioconjugates would become an alternative candidate for sandwich-type immunoassay to obtain much greater signal amplification for the following experiments.

3.6. The performance of the ECL immunosensor

3.6.1. Calibration curve

On the basis of the optimal condition, the quantitative range of the proposed ECL immunosensor was explored by using the developed sandwich-type format with Pd&PtNPs@rGO–GOD–Ab_2 bioconjugates as the tracer and luminol together with glucose as the substrate. As a result, the ECL signal increased with the increasing concentration of CEA in the range from 0.0001 ng mL^{-1} to 160 ng mL^{-1} and a linear relationship appeared to the logarithm of CEA concentration (Fig. 5). The linear equation was $I_{ECL}=4207.60+880.43\ \log(c_{CEA})$ with a correlation coefficient of 0.9993 and an evaluated detection limit of 0.03 pg mL^{-1} (S/N=3). Compared with other CEA immunosensors shown in Table S1, the proposed immunosensor exhibited much higher sensitivity or wider response range. The reason may be as follows: plenty of GOD was conjugated onto the surface of Pd&PtNPs@rGO, which could significantly bioelectrocatalyze glucose to in situ produce H_2O_2. Meanwhile, in turn Pd&PtNPs could catalyze H_2O_2 to generate various ROSs, which could accelerate the reaction of luminol to form 3-aminophthalate anions at the excited state and then enhance the luminol ECL intensity and improve the sensitivity of the immunosensor. Thus, this procedure can be employed for highly sensitive quantification of CEA.

3.6.2. Stability, reproducibility and selectivity

The ECL stability of the proposed immunosensor was also examined by monitoring of its ECL response toward 1 ng mL^{-1}

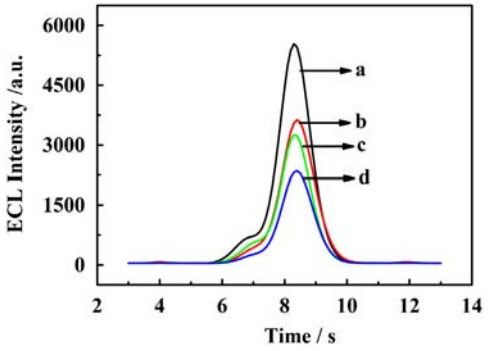

Fig. 4. The comparison of different labeled probes: Pd&PtNPs@rGO–GOD–Ab_2 bioconjugates (a), PdNPs@rGO–GOD–Ab_2 bioconjugates (b), PtNPs@rGO–GOD–Ab_2 bioconjugates (c) and rGO–GOD–Ab_2 bioconjugates (d).

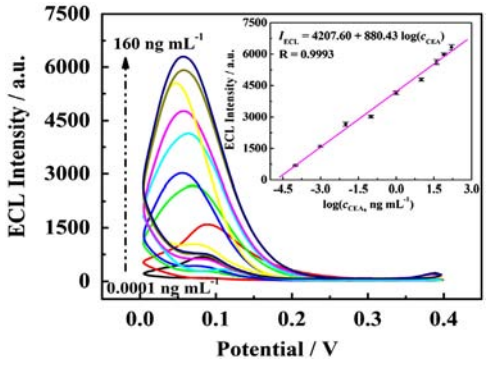

Fig. 5. ECL responses of the proposed immunosensor to different concentrations of CEA (ng mL^{-1}): 0.0001, 0.001, 0.01, 0.1, 1, 10, 40, 80, 160. Inset: calibration curve for CEA assay in PBS (pH 7.4) containing 1×10^{-4} M luminol and 0.01 M glucose.

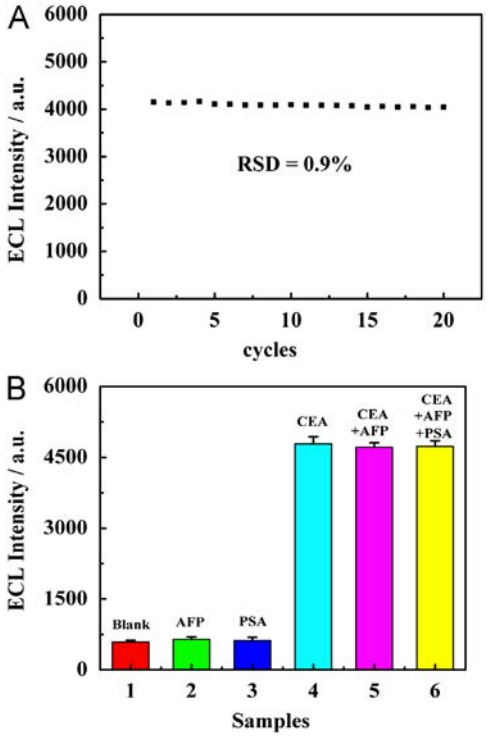

Fig. 6. (A) The stability of the proposed ECL immunosensor incubated with 1 ng mL^{-1} CEA under consecutive cyclic potential scans for 20 cycles. (B) The specificity of the proposed ECL immunosensor. All working buffers were 0.1 M PBS (pH 7.4) containing 1×10^{-4} M luminol and 0.01 M glucose.

CEA antigen under consecutive cyclic potential scans for 20 cycles and the result is presented in Fig. 6A. It was found that the response of the ECL immunosensor did not show obvious changes. The long-term stability of the immunosensor was also investigated. The ECL responses of the as-prepared immunosensor were recorded every 10 days in a period of 30 days of storage at 4 °C. The developed ECL immunosensor maintained 96.3% of its initial ECL signal after 10 days and 89.6% after 30 days. The results indicated that the proposed immunosensor exhibited satisfying stability both in a short time and over a long time. The preeminent stability may originate from the following reasons: firstly, the DpAu/CNTs–Gra membrane provided an outstanding matrix with large specific surface area and good biocompatibility for catching of Ab_1. In addition, Pd&PtNPs@rGO composites provided good electron transfer tunnel and strong catalytic effect for catalyzing glucose to in situ generate H_2O_2, which in turn was changed to various ROSs promoting the luminol ECL catalyzed by Pd&PtNPs. Otherwise, the coreactant, H_2O_2, produced by catalyzing glucose at the surface of the modified electrode, can maintain the amount of H_2O_2 in time around the immunosensor.

Selectivity is an important criterion for immunosensors. Therefore the interference experiment was studied by detecting the ECL response of the proposed immunosensor by incubating with interference samples under the same experimental conditions. The ratio between the target analyte and the interferent was 1:10. As shown in Fig. 6B, no target protein, such as AFP (100 ng mL^{-1}), PSA (100 ng mL^{-1}), no apparent change of the ECL intensity was observed compared with that of testing blank solution. Furthermore, the ECL signals of the mixed incubating solution (one contained 10 ng mL^{-1} CEA and 100 ng mL^{-1} AFP; and the other was composed of 10 ng mL^{-1} CEA, 100 ng mL^{-1} AFP and 100 ng mL^{-1} PSA) presented neglectable changes compared with that of determination of CEA only. Thus, the proposed immunosensor had good selectivity and specificity to CEA and this made it feasible for the determination of CEA.

The reproducibility of the immunoassay was investigated by using the intra- and inter-assays precision. The intra-assay precision was evaluated by testing the 0.01 ng mL^{-1} CEA for three reduplicate measurements. The inter-assay precision or reproducibility was investigated with the ECL responses of 40 ng mL^{-1} CEA using three immunosensors made at the same GCE with various batches. The relative standard deviations (R.S.D.) of the intra- and inter-assay were 4.9% and 7.7%, respectively, which indicated an acceptable precision and fabrication reproducibility of the proposed immunoassay.

3.6.3. Application

The feasibility of the ECL immunoassay system for clinical applications was investigated by the standard addition method (adding CEA of different standard concentrations to normal human serum samples). We found that the recovery was acceptable ranging from 95.8% to 108.9%. To further evaluate the analytical reliability and application potentials of the developed immunosensor, clinical serum samples were analyzed by the proposed ECL immunosensor, and the obtained results were compared with commercially enzyme-linked immunosorbent assay (ELISA) as shown in Table 1. In addition, we also made a comparative study of the recovery using the developed method and ELISA. 10 ng mL^{-1} of CEA was added into corresponding serum samples, and the results were compared with ELISA as shown in Table 1. It obviously indicated that the proposed immunosensor is in good agreement with ELISA. Thus, the proposed ECL immunosensor may provide an alternative strategy for analytical application in real biological samples.

4. Conclusion

We have successfully developed a novel sandwich-type luminol cathodic ECL immunosensor for ultrasensitive detection of CEA.

Table 1
CEA determination in serum and the recovery by two methods.

Serum samples	1	2	3
Proposed immunosensor (ng mL^{-1})[a]	2.31	3.58	5.15
ELISA (ng mL^{-1})[a]	2.15	3.42	5.37
Relative deviation (%)	7.44	4.68	−4.09
Spiked (ng mL^{-1})	10.0	10.0	10.0
Proposed immunosensor (ng mL^{-1})[a]	12.66	13.35	15.38
Recovery (%)	103.5	97.7	102.3
ELISA recovery (%)	98.2	105.4	96.2
Relative deviation (%)	5.40	−7.31	6.34

[a] The values shown here are the average values from three measurements.

The higher sensitivity and wider linear range of the proposed immunosensor should be taken into account for the following reasons: firstly, AuNPs electrodeposited on CNTs–Gra composites modified electrode not only facilitated electron transfer but also provided large biocompatible surface area for the immobilization of abundant Ab_1. Secondly, rGO with a high aspect ratio could increase the amount of Pd&PtNPs, thus further enhancing the loading amount of GOD. Consequently, amplified cathodic ECL of luminol signals was obtained by the efficient catalysis of GOD toward glucose to in situ production of H_2O_2 as coreactant. Then Pd&PtNPs catalyzed H_2O_2 to generate various ROSs, which accelerated the cathodic ECL reaction of luminol and then enhanced the luminol cathodic ECL intensity and improved the sensitivity and stability of the immunosensor. Besides, although the proposed ECL immunosensor was applied for the determination of CEA, it also provided excellent opportunities for other targets.

Acknowledgments

This work was financially supported by the NNSF of China (21075100), State Key Laboratory of Electroanalytical Chemistry (SKLEAC2010009), Ministry of Education of China (Project 708073), Natural Science Foundation of Chongqing City (CSTC-2009BA1003, CSTC-2010BB4121, CSTC-2011BA7003), Specialized Research Fund for the Doctoral Program of Higher Education (20100182110015) and the Postgraduate Science and Technology Innovation Program of Southwest China University (Grant no. KB2010006).

Appendix A. Supporting information

Supplementary information associated with this article can be found in the online version at http://dx.doi.org/10.1016/j.talanta.2013.03.018.

References

[1] F. Liu, Y. Zhang, S.G. Ge, J.J. Lu, J.H. Yu, X.R. Song, S. Liu, Talanta 99 (2012) 512–519.
[2] Z.Y. Guo, T.T. Hao, J. Duan, S. Wang, D.Y. Wei, Talanta 89 (2012) 27–32.
[3] R.X. Duan, X.M. Zhou, D. Xing, Anal. Chem. 82 (2010) 3099–3103.
[4] Y.S. Guo, X.P. Jia, S.S. Zhang, Chem. Commun. 47 (2011) 725–727.
[5] X. Zhu, L.F. Chen, Z.Y. Lin, B. Qiu, G.N. Chen, Chem. Commun. 46 (2010) 3149–3151.
[6] Z.Y. Guo, P.P. Gai, Anal. Chim. Acta 688 (2011) 197–202.
[7] H.Y. Yang, Y.Q. Wang, H.L. Qi, Q. Gao, C.X. Zhang, Biosens. Bioelectron. 35 (2012) 376–381.
[8] M.M. Richter, Chem. Rev. 104 (2004) 3003–3036.
[9] W.J. Miao, Chem. Rev. 108 (2008) 2506–2553.
[10] X. Cai, J.L. Yan, H.H. Chu, M.S. Wu, Y.F. Tu, Sens. Actuators B: Chem. 143 (2010) 655–659.
[11] S.J. Xu, Y. Liu, T.H. Wang, J.H. Li, Anal. Chem. 82 (2010) 9566–9572.
[12] X.H. Wei, C. Liu, Y.F. Tu, Talanta 94 (2012) 289–294.
[13] S. Kulmala, T. Ala-Kleme, A. Kulmala, D. Papkovsky, K. Loikas, Anal. Chem. 70 (1998) 1112–1118.
[14] J. Wang, R.R. Zhao, M.Z. Xu, G.N. Chen, Electrochim. Acta 56 (2010) 74–79.
[15] H. Dai, Y.Y. Lin, G.F. Xu, L.S. Gong, C.P. Yang, X.L. Ma, G.N. Chen, Electrochim. Acta 78 (2012) 508–514.
[16] L.L. Li, K.P. Liu, G.H. Yang, C.M. Wang, J.R. Zhang, J.J. Zhu, Adv. Funct. Mater. 21 (2011) 869–878.
[17] K.S. Novoselov, A.K. Geim, S.V. Morozov, D. Jiang, Y. Zhang, S.V. Dubonos, I. V. Grigorieva, A.A. Firsov, Science 306 (2004) 666–669.
[18] D.R. Dreyer, R.S. Ruoff, C.W. Bielawski, Angew. Chem. Int. Ed. 49 (2010) 9336–9345.
[19] C.N.R. Rao, A.K. Sood, K.S. Subrahmanyam, A. Govindaraj, Angew. Chem. Int. Ed. 48 (2009) 7752–7777.
[20] M.J. Allen, V.C. Tung, R.B. Kaner, Chem. Rev. 110 (2010) 132–145.
[21] S.J. Xu, Y. Liu, T.H. Wang, J.H. Li, Anal. Chem. 83 (2011) 3817–3823.
[22] Y.P. Dong, J.Z.Y. Ding, X.F. Chu, W.B. Zhang, J. Electrochem. Soc. 159 (2012) 692–696.
[23] H.F. Yang, C.S. Shan, F.H. Li, D.X. Han, Q.X. Zhang, L. Niu, Chem. Commun. 26 (2009) 3880–3882.
[24] W. Wang, E.M. Goh, K.K. Manga, Q. Bao, P. Yang, K.P. Loh, ACS Nano 4 (2010) 6180–6187.
[25] S. Stankovich, D.A. Dikin, G.H.B. Dommett, K.M. Kohlhaas, E.J. Zimney, E. A. Stach, R.D. Piner, S.T. Nguyen, R.S. Ruoff, Nature 442 (2006) 282–286.
[26] E. Bekyarova, M.E. Itkis, P. Ramesh, C. Berger, M. Sprinkle, W.A. de Heer, R. C. Haddon, J. Am. Chem. Soc. 131 (2009) 1336–1337.
[27] S.Y. Yang, K.H. Chang, Y.F. Lee, C.C.M. Ma, C.C. Hu, Electrochem. Commun. 12 (2010) 1206–1209.
[28] T.Y. You, O. Niwa, M. Tomita, S. Hirono, Anal. Chem. 75 (2003) 2080–2085.
[29] H. Niu, R. Yuan, Y.Q. Chai, L. Mao, Y.L. Yuan, Y.L. Cao, Y. Zhuo, Chem. Commun. 47 (2011) 8397–8399.
[30] L.Y. Cao, Y.L. Liu, B.H. Zhang, L.H. Lu, ACS Appl. Mater. Interfaces 2 (2010) 2339–2346.
[31] S.Y. Deng, J.P. Lei, L.X. Cheng, Y.Y. Zhang, H.X. Ju, Biosens. Bioelectron. 26 (2011) 4552–4558.